Applied Catalysis B: Environmental 134–135 (2013) 258–264

Contents lists available at SciVerse ScienceDirect

Applied Catalysis B: Environmental

journal homepage: www.elsevier.com/locate/apcatb

Hydrothermal activation of silver supported alumina catalysts prepared by sol–gel method: Application to the selective catalytic reduction (SCR) of NOx by *n*-decane

Carolina Petitto [a,b,c], Hubert P. Mutin [a,c], Gérard Delahay [a,b,*]

[a] Institut Charles Gerhardt Montpellier, UMR 5253 CNRS/ENSCM/UM2/UM1, France
[b] Matériaux Avancés pour la Catalyse et la Santé, 8 rue de l'Ecole Normale, 34296 Montpellier Cedex 5, France
[c] Chimie Moléculaire et Organisation du Solide, Université Montpellier 2, Place Eugène Bataillon, 34095 Montpellier Cedex 5, France

ARTICLE INFO

Article history:
Received 10 December 2012
Received in revised form 10 January 2013
Accepted 14 January 2013
Available online 26 January 2013

Keywords:
Hydrothermal activation
Sol–gel catalysts
HC-SCR
Nitrogen monoxide
n-Decane
Supported alumina
Silver

ABSTRACT

2 wt% Ag– and 2 wt% Ag–1.5 wt% Nb mesoporous alumina catalysts were prepared by non-hydrolytic sol–gel process. Silver accessibility is enhanced by calcination at high temperature. By performing calcination in presence of water vapour, silver particles are well dispersed and interact more strongly with the alumina surface and activity in *n*-decane-SCR of NOx is greatly improved. Moreover, the addition of niobium in the starting material leads to more efficient catalysts and enhances mainly the low temperature activity.

1. Introduction

Reduction of nitrogen oxides by hydrocarbons (HC-SCR) is still a highly desirable technology for the NOx removal if a suitably active commercial catalyst is developed [1,2]. Since the first studies, in the 1990s, on silver/alumina materials [3–5], this catalytic system remains a very promising candidate for the HC-SCR of NOx [6]. It must be underlined that this system is selective under conditions close to those of an exhaust gas and long chain hydrocarbons can provide higher NOx conversion efficiencies [7–10], if are not limited by deactivation. High yields in NOx removal are also achieved, with this kind of catalyst, when oxygen-containing organic compounds (ethanol) are used as reductants [3,11–16]. The optimal silver content, for obtaining the best efficiency for conventional impregnated catalysts, is in the 1.5–3 wt% window, depending on the alumina starting material. [3,11,17–22]. Moreover, the preparation method, including the calcination step, is crucial [21,23–26] because it influences the nature of the silver species present, i.e. isolated species, silver aluminate, nanosized Ag_2O clusters, $Ag_n^{\delta+}$ clusters or large metallic Ag^0 clusters. It is widely believed that highly dispersed silver ions, strongly interacting with Al_2O_3 or silver particles with a low oxidation state (within silver oxide- or aluminate type entities interacting with the alumina support) [27–30], are efficient for this reaction [11,17,31] showing the importance of the type of alumina used [32]. On the other hand when metallic silver particles or Ag_n^0 clusters are dominant in the high-silver content alumina catalysts, the resulting catalysts are less selective for NO reduction but are very active for the direct combustion of hydrocarbons [11,19,22,29,33,34].

Various preparation techniques of Ag/alumina catalysts were attempted for improving the HC-SCR catalytic activity [8,17,19,23,34–36]. The improvement of the Ag/Al_2O_3 formulation can be also realised through the addition of an element which can increase the adequate properties of the solid necessary for the SCR reaction (acidity, oxidation, stability, etc.) [37–39]. In particular, from a study on the nature of alumina as support, Sultana et al. [40] argued that the reaction of NO reduction with long chain hydrocarbons over Ag/Al_2O_3 can be significantly enhanced by tuning acidity and pore size distribution of the support. Therefore, our interest went towards niobium as it is known to increase the thermal stability and also the acidic properties of alumina [41,42]. Moreover, from our preliminary results [43] where the effect of addition of silicon, titanium and niobium to alumina was compared, the best HC-SCR activity was obtained with niobium.

* Corresponding author. Tel.: +33 0467163480; fax: +33 04 67163470.
E-mail address: gerard.delahay@enscm.fr (G. Delahay).

0926-3373/$ – see front matter © 2013 Published by Elsevier B.V.
http://dx.doi.org/10.1016/j.apcatb.2013.01.018

The catalysts used in this study were prepared by Non-Hydrolytic Sol–Gel (NHSG) process. This process offers the possibility to obtain homogeneous mesoporous materials in a simple way at laboratory scale [44–46]. Synthesis of our catalysts, Ag(Nb)/Al_2O_3, was derived from the method described for alumina reported by Acosta et al. [47]. Schematically the preparation proceeds according to the following equation:

$$AgCl + Nb_2Cl_5 + ((CH_3)_2CH)_2O \xrightarrow[383\,K]{CH_2Cl_2} AgNbAlO_x \quad (1)$$

followed by adequate thermal activation [48]. This last step is required since it should facilitate the migration of silver towards the surface of alumina [48]. The objectives of this study are to show the effect of niobium addition and to define the role of water vapour added during the thermal treatment.

2. Experimental

2.1. Catalyst preparation

2.1.1. Preparation of Ag_{CAL823} (2 wt% Ag)

0.0664 g of silver chloride and 6.400 g of aluminium chloride are added, under inert atmosphere, to a solution of dichloromethane (10 cm^3) and isopropyl ether (10.2 cm^3). Then the reaction mixture was charged into a stainless steel autoclave equipped with a glass liner. The autoclave is then placed into the drying oven and kept at 383 K for 6 days. After this ageing, the gel was washed with CH_2Cl_2 and dried under vacuum firstly at room temperature and then at 393 K. The sample was calcined at 823 K under airflow for 8 h.

2.2. Preparation of $AgNb_{CAL823}$ (2 wt% Ag–1.5 wt% Nb)

0.0664 g of silver chloride, 0.127 g of niobium chloride and 6.234 g of aluminium chloride are added, under inert atmosphere, to a solution of dichloromethane (10 cm^3) and isopropyl ether (10.1 cm^3). Then the same protocol as that applied to the preparation of Ag_{Cal823} was used.

2.3. Thermal treatment

1 g of Ag_{CAL823} or 1 g of $AgNb_{CAL823}$ are set on a porous frit of a U tube quartz reactor in which airflow of 50 cm^3/min passes through. Then, the reactor is heated at a temperature T (T > 823 K) with a ramp of 6 K/min and kept at this temperature for 16 h and then cooled to room temperature. The samples were labelled Ag_{CALT} or $AgNb_{CALT}$. Calcinations at a temperature T (T > 823 K) with addition of water in the calcining gas were also done and the samples were labelled Ag_{HDTT} or $AgNb_{HDTT}$. The injection of $H_2O_{(liq.)}$ (0.0041 cm^3/min), by a syringe-pump, is started during the ramp of temperature when the temperature of the sample is around 373 K. The injection of water is stopped during the cooling of the furnace once the temperature is below 673 K.

2.4. Catalytic activity studies

The SCR of NO by *n*-decane was performed in a flow reactor operating at atmospheric pressure. An aliquot (0.040 g) of the powdered catalyst was placed in a reactor and pretreated in situ at 823 K for 1 h in air. After cooling to 473 K, the reaction was performed using a gas mixture containing 0.04 vol% NO (purity > 99.995%), 0.02 vol% *n*-decane (purity > 99.5%), 2.5 vol% H_2O (purity > 99.5%) and 8 vol% O_2 (purity > 99.995%), the balance with helium. Thus, under our experimental conditions, the ratio HC/NOx (carbon number × vol% HC/vol% NOx) is 5. The total flow rate was 6000 cm^3/h, leading to a WHSV space velocity (total flowrate/sample amount) of 150,000 $cm^3\,g^{-1}\,h$. The temperature was varied from 473 to 823 K with a ramp of 5 K/min. The composition of the effluents was monitored continuously by sampling on line to a quadrupole mass spectrometer (Pfeiffer Vacuum) equipped with Faraday and SEM detectors (0–200 amu) and following the masses 28, 30, 44, 46, and 57. The possible N_2O and CO formations were checked by analysing the outlet gas with a two module micro gas chromatograph (CP-4900 Micro-GC Varian), each module being equipped with a thermal conductivity detector (TCD). The first module has a 5 Å molecular sieve column, allowing the analysis of $O_2/N_2/CO/CH_4$ and a back flush system to send the heavy products and CO_2 towards the second module. The latter has a PORAPLOT Q column in order to separate CO_2 and N_2O. With the CP-4900 μGC, a sample analysis of the gas phase, which injection is performed through a system capillary/micro-pump, can be realised every 20 K.

2.5. Catalyst characterization

2.5.1. Adsorption–desorption of nitrogen

The textural properties, surface area and porosity, of calcined samples were obtained from nitrogen adsorption–desorption isotherms measured at 77 K by using a Micromeritics Asap 2000 Analyser. Before the nitrogen adsorption measurement, the samples were outgassed at 523 K until a static vacuum of 3×10^{-5} bar was reached. BET method was used to calculate the specific surface area. Pore volumes were calculated at the end of the step corresponding to the filling of the pores. Pore diameter was evaluated from the nitrogen desorption branch according to the BJH model.

2.6. X-ray diffraction (XRD)

Powder X-ray diffraction data were obtained on a Brüker AXS D8 diffractometer by using Cu Kα radiation and a Ni filter.

2.7. X-ray photoelectron spectroscopy (XPS)

The relative presence of Ag and Nb on the surface was estimated from XPS measurements on a 250 Thermo Electron ESCALAB device by calculating the area ratio: $Ag3d_{3/2}/Al2p_{3/2}$ and $Nb3d_{5/2}/Al2p_{3/2}$.

2.8. Transmission electron microscopy (TEM)

TEM images were collected on a JEOL 1200 EX II (80–100 kV) microscope.

2.9. NH_3-temperature programmed desorption (NH_3-TPD)

Total acidity measurement was evaluated by NH_3-TPD using an AUTOCHEM2910 (Micromeritics). Before NH_3 adsorption, the samples were pre-treated under air flow (30 cm^3/min) at 823 K (ramp 10 K/min) for 2 h. NH_3 adsorption was done at 373 K by exposition to 5 vol% NH_3 in He (flow rate = 30 cm^3/min) for 45 min and then flushed with He (30 cm^3/min) during 2 h to remove the physisorbed ammonia. Finally, ammonia was desorbed in helium flow (30 cm^3/min) from 373 K to 923 K using a heating rate of 10 K/min.

3. Results and discussion

3.1. Catalytic results

NO and *n*-decane conversion profiles versus temperature of Ag_{CAL823} and $AgNb_{CAL823}$ are reported in Fig. 1. These two catalysts, prepared by NHSG, show similar conversion profiles. NOx reduction and *n*-decane conversions begin simultaneously at 573 K and 613 K, for Ag_{CAL823} and $AgNb_{CAL823}$, respectively. The reduction of NO reaches its maximum at ≈723 K, it is followed by a plateau and

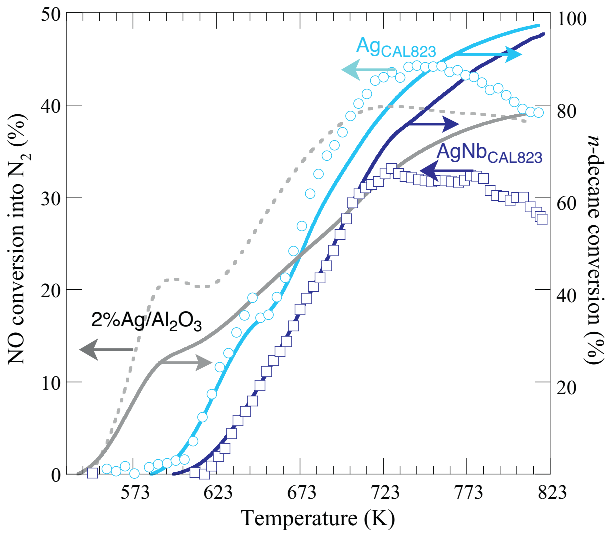

Fig. 1. Reaction temperature dependence of NO conversion (marker) and *n*-decane conversion (full line) over Ag_{CAL823} (○ ; ▬▬), $AgNb_{CAL823}$ (□ ; ▬▬) and 2%Ag/Al2O3 (▪ ▪ ▪ ; ▬▬) prepared by impregnation. Total flowrate = 6 L h-1, catalyst amount = 40 mg, [*n*-decane] = 0.02%, [NO] = 0.04%, $[H_2O]$ = 2.50%, $[O_2]$ = 8.00% O_2 and balance with helium.

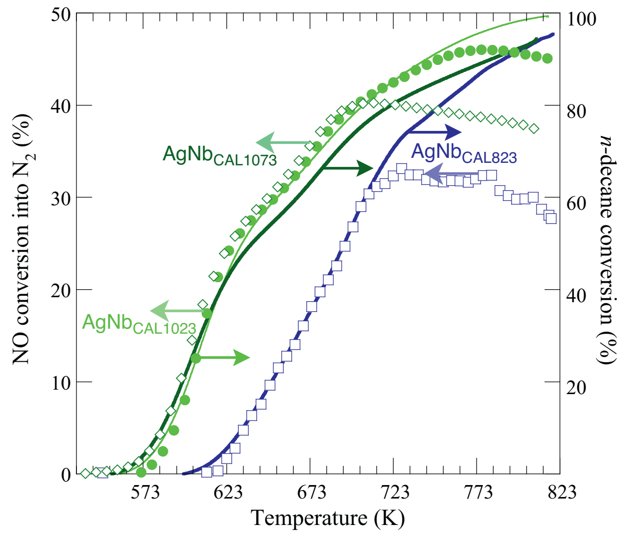

Fig. 2. Reaction temperature dependence of NO conversion (marker) and *n*-decane conversion (full line) over $AgNb_{CAL823}$ (□ ; ▬▬), $AgNb_{CAL1023}$ (● ; ▬▬) and AgNbCAL1073 (◇ ; ▬▬). Test conditions: see Fig. 1.

then by a slow decrease over 783 K. For *n*-decane, the conversion increases progressively up to near 100% conversion at 823 K. These two catalysts are less efficient than a conventional 2% Ag/Al_2O_3 prepared by classical impregnation and a slight higher activity is obtained with the catalyst without niobium. This lowest activity can be explained by the lack of accessible silver due to the method of preparation used. Hence sol–gel method starting from alumina and silver precursors is not the best method for obtaining catalysts where all of the silver is supported on the alumina surface. Moreover, HC-SCR of NOx on silver alumina catalysts, prepared by impregnation, is very sensitive to the silver content. By considering the Tamann temperature of silver [49], calcination, above 823 K, could activate and accelerate the migration of the totality of the silver species at the surface of alumina. Moreover by increasing the calcination temperature, the migration of niobium oxide towards the surface should also be enhanced. Therefore $AgNb_{CAL823}$ was calcined at 1023 and 1073 K, respectively. The NO conversion profiles obtained on these two solids were shifted towards the low temperature (Fig. 2). NO reduction activity starts at 583 K followed by a more rapid increase of the conversion compared with the calcined samples at 823 K. Nevertheless, $AgNb_{CAL1023}$ shows a better activity in NO reduction than $AgNb_{CAL1073}$, at high temperatures, with an additional NO conversion of around 10% above 723 K. This result shows the need for treating the solids at high temperatures. We can suggest that a highest temperature of calcination favours a better migration of silver species towards the surface of alumina. On the other hand, up to 1023 K, the migration of niobium oxide should still be very weak or absent; but it will be more important at 1073 K and could justify the difference of activity observed at higher temperatures.

According to Nakatsuji et al. [50], the calcination of silver impregnated alumina in presence of water vapour at high temperature promotes the formation of $AgAlO_2$ on the alumina surface; these silver species were supposed to be the active species in the HC-SCR of NO. Therefore, we applied a hydrothermal treatment to Ag and AgNb catalysts prepared by NHSG. The presence of water vapour in the calcination gas allows to obtain catalysts much more active at low temperature. The best result is achieved with the catalyst $AgNb_{CAL823}$ hydrotreated at 1023 K (Fig. 3).

It should be pointed out that in absence of niobium, the effect of hydrotreatment is optimal with a treatment temperature at 1023 K or 1073 K but the catalytic efficiency remains lower than that obtained with $AgNb_{HDT1023}$ (Fig. 4). Thus the addition of niobium and the calcination of the solid with H_2O_g at 1023 K are required to produce a highly active catalyst, issued from sol–gel process, in a very large range of temperatures. These two results have motivated the comparative characterization, described below, of the catalysts which activity is shown in Fig. 4. First of all, we have focussed on the catalyst properties evolution with the thermal and hydrothermal temperature treatment. We have checked by XPS if the alumina surface is enriched in silver after a treatment at a higher temperature. Finally, the size distribution of silver particles and the acidic properties of the catalysts were evaluated from TEM and NH_3-TPD respectively.

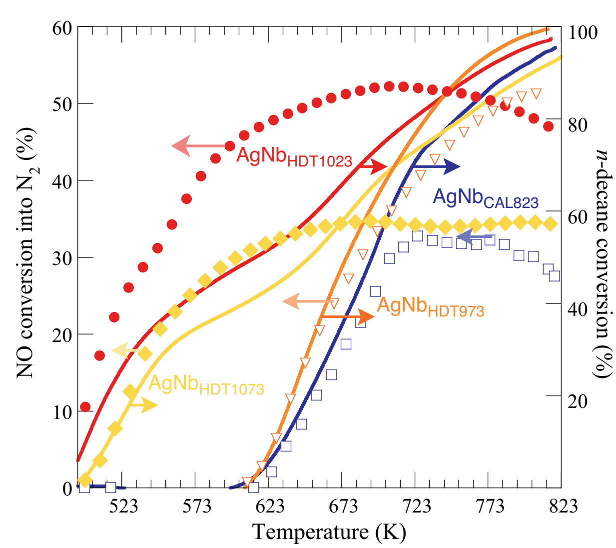

Fig. 3. Reaction temperature dependence of NO conversion (marker) and *n*-decane conversion (full line) over $AgNb_{CAL823}$ (□ ; ▬▬), AgNbHDT973 (▽ ; ▬▬), $AgNb_{HDT1023}$ (● ; ▬▬) and AgNb HDT1073 (◆ ; ▬▬). Test conditions: see Fig. 1.

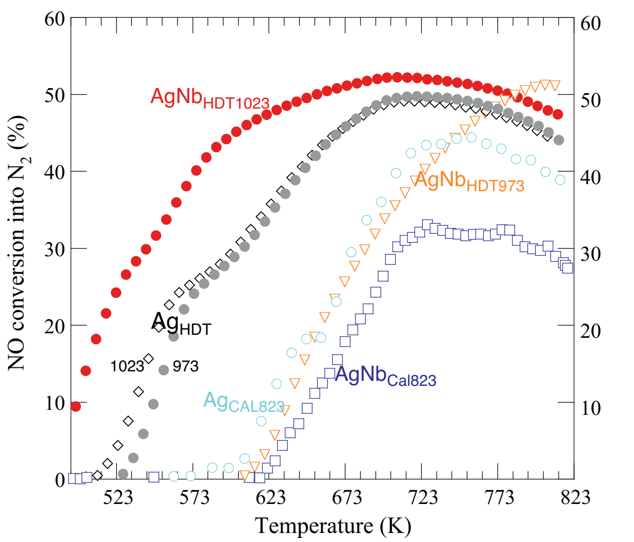

Fig. 4. Reaction temperature dependence of NO conversion over AgNb$_{CAL823}$ (□), AgNbHDT973 (▽), AgNb$_{HDT1023}$ (●), Ag$_{CAL823}$ (○), AgHDT973 (●) and Ag$_{HDT1023}$ (◇). Test conditions: see Fig. 1.

3.2. Catalyst characterization

3.2.1. S_{BET} and porosity

Some nitrogen sorption isotherms of Ag and AgNb materials are shown in Fig. 5, revealing a type IV isotherm (defined by IUPAC) [51], typical of mesoporous materials. The specific surface area is up to 346 $m^2\,g^{-1}$ when the synthesized material containing niobium, was calcined at 823 K, whereas 283 $m^2\,g^{-1}$ is obtained without niobium (Table 1). When the sample calcined at 823 K was further calcined at higher temperature, the BET surface area is reduced which can be ascribed to the appearance of a more ordered transition alumina phase (gamma-alumina). This decrease is always stronger in presence of water in the calcination gas and, this loss of surface area was much more important for the materials with niobium. However, the isotherms have the same shape as that of the one calcined at 823 K, revealing the excellent thermal stability of the alumina based samples. The pore sizes have narrow distribution which, depending from the material, varied over the ranges from 4.5 to 8.0 nm or 9.5 to 12.0 nm and are centred at the values reported in Table 1, indicating that the mesoporous based alumina materials have an uniformity of pore size and an ordered mesostructure. The surface areas of Ag$_{HDT1023}$ and AgNb$_{HDT1023}$ were similar and remained acceptable for catalysis considering the severity of the hydrothermal treatment.

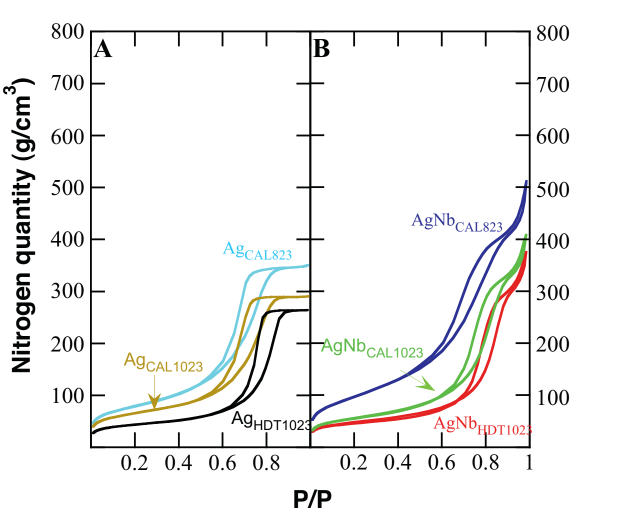

Fig. 5. N2 adsorption–desorption isotherms of: (A) Ag$_{CAL823}$ (cyan line), Ag$_{CAL1023}$ (gold line), Ag$_{HDT1023}$ (black line) and (B) AgNb$_{CAL823}$ (blue line), AgNb$_{CAL1023}$ (green line), AgNb$_{HDT1023}$ (red line).

Table 1
Textural properties of the catalysts.

Catalysts	Textural properties		
	S_{BET} ($m^2\,g^{-1}$)	ϕ_{pores} (nm)	V_p ($cm^3\,g^{-1}$)
Ag$_{CAL823}$	283	5.5	0.54
Ag$_{CAL1023}$	240	5.7	0.45
Ag$_{HDT973}$	187	7.1	0.44
Ag$_{HDT1023}$	162	7.4	0.41
AgNb$_{CAL823}$	346	6.9	0.80
AgNb$_{CAL1023}$	204	9.0	0.63
AgNb$_{CAL1073}$	213	8.7	0.60
AgNb$_{HDT973}$	167	10.6	0.66
AgNb$_{HDT1023}$	167	11.0	0.58

3.2.2. XRD analysis

Ag and AgNb alumina materials were almost amorphous after calcination for 8 h at 823 K (Fig. 6A). As expected, after heating at higher temperatures, a better crystallization of γ-alumina was observed. The presence of niobium in the solid (Fig. 6A) or water in the calcination gas (Fig. 6B AgNb for example) seems to delay the observed crystallization. No diffraction peaks corresponding to metallic silver, silver oxide or niobium oxide and or silver aluminate were detected. It was recently ruled out by Korhonen et al. [7] that silver aluminate is the active phase for the SCR reaction. They have proposed that the active silver species, present on the alumina support, are 2-dimensional oxidized Ag_n^+ species.

3.2.3. Silver migration determined from XPS spectroscopy

The sol–gel processes are not ideal for preparing supported catalysts since it is expected that a very important part of the element to be supported remains inaccessible in the core of the material. Firstly, it is known that silver oxides are inherently unstable. The stoichiometric oxides AgO and Ag_2O decompose at 373 and 503 K, respectively. Secondly, an important physical characteristic of silver is that it has a Tamman temperature (T_{Tamman} (K) ≈ 0.5 × T_{melt} (K)) of 617 K which suggests that bulk silver atoms tend to move at relatively low temperatures and thus migration of silver to the alumina surface should occur easily. Since niobium oxide has a T_{Tamman} of 892 K, its diffusion towards the surface will be much more difficult, and will require higher temperatures. Treatment at 1023 K allows a greater enrichment in both silver and niobium, as shown by the increase of surface ratio ($Ag3d_{3/2}/Al2p_{3/2}$ and $Nb3d_{5/2}/Al2p_{3/2}$) measured by XPS (Table 2). Unfortunately, our XPS analyses have not allowed a determination of the average oxidation state of silver of the silver alumina samples since the XPS spectrum of Ag_2O

Table 2
Ag/Al and Nb/Al relative surface ratio and acidic properties of some catalysts.

Catalysts	Metal surface ratio[a]		Acidic properties[b]	
	Ag/Al	Nb/Al	NH_3 (μmol g^{-1})	Site density (μ mol/m^2)
Ag$_{CAL823}$	4.7		600	2.12
Ag$_{CAL1023}$	8.4		525	2.19
Ag$_{HDT1023}$	8.8		440	2.72
AgNb$_{CAL823}$	6.8	8.9	710	2.05
AgNb$_{CAL1023}$	10.4	12.2	520	2.55
AgNb$_{HDT1023}$	10.2	12.7	480	2.87

[a] The relative presence of Ag and Nb was evaluated from XPS measurements.
[b] Total acidity measurement was evaluated by NH_3-TPD.

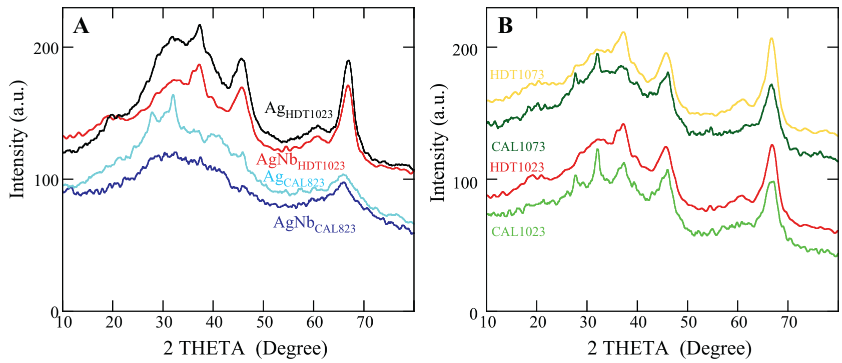

Fig. 6. XRD patterns of: (A) $AgNb_{CAL823}$ ( ), Ag_{CAL823} ( ), $AgNb_{HDT1023}$ ( ), $Ag_{HDT1023}$ ( ) and (B) $AgNb_{CAL1023}$ ( ), $AgNb_{HDT1023}$ ( ), AgNbCAL1073 ( ), $AgNb_{HDT1023}$ ( ).

had evolved, during the analysis, and the resulting spectrum was similar to the XPS spectrum of metallic silver.

3.2.4. Silver particle size determined from TEM

The particle size distribution was determined by randomly measuring the size of 500 particles on different TEM images. The silver particle size distribution (Fig. 7) on the surface of the different samples is quite broad: from 3 nm to 70 nm (particles below 3 nm were not detectable), except for $AgNb_{HDT1023}$. On the latter catalyst, the size distribution is narrow with a size of silver particles in the range 3–22 nm but with also the presence of larger particles. The hydrothermal treatment has not totally the same incidence on the silver dispersion. On the catalyst without niobium, it does improve the silver particle size distribution but very large particles (30 nm ≤ diameter ≤ 70 nm) are also present. On the other hand, on the solid with niobium, the silver dispersion is largely enhanced.

Moreover it seems that the calcination in absence of water up to 1023 K has no significant effect on the size distribution suggesting that the role of the temperature is only to promote the migration of silver to the surface.

3.2.5. Acidic properties

The acidic properties of the catalysts were evaluated from ammonia temperature programmed desorption (NH_3-TPD). The NH_3-TPD curves were fitted by Gaussian deconvolution to obtain the acid site distribution (Fig. 8). Three peaks with maxima in 453–473 K, 523–593 K and 720–795 K temperature ranges were observed in the NH_3-TPD curves which can be assigned to the NH_3 desorption from weak, medium and strong acid sites, respectively. The highest quantity of desorbed ammonia was observed for calcined materials and in particular for $AgNb_{CAL823}$ (Table 2). The addition of niobium increases the strength of acid sites and, the proportion of medium acid sites is predominant (Fig. 8). A strong

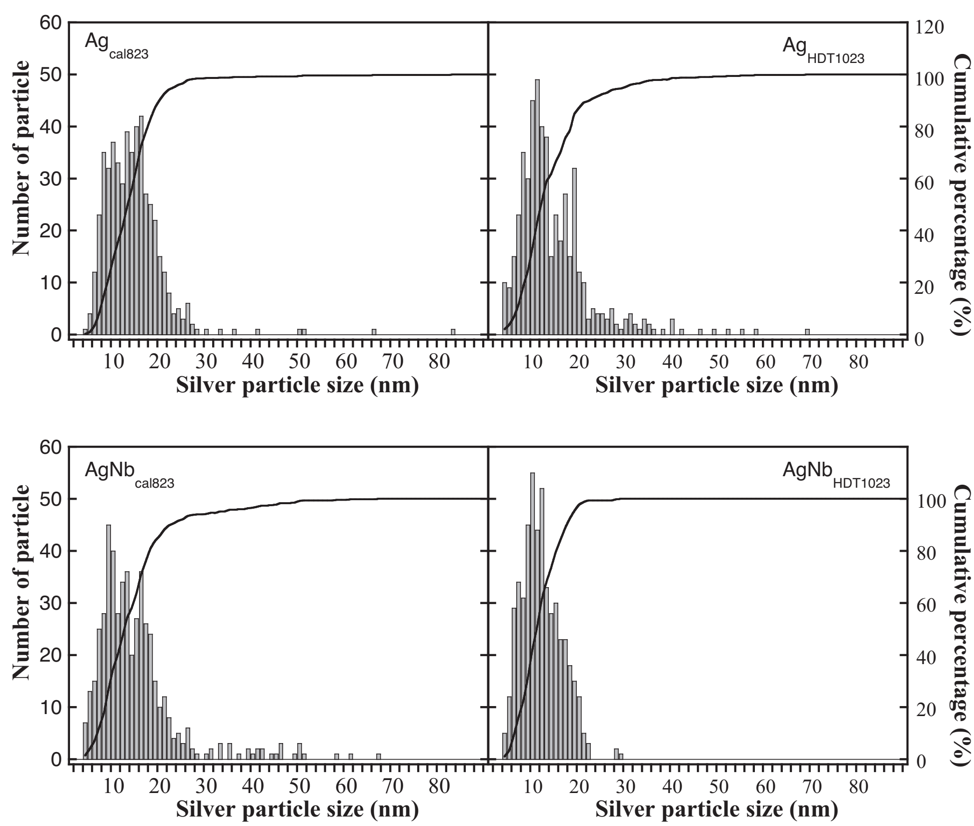

Fig. 7. Histograms presenting particle size distribution for Ag_{CAL823}, $Ag_{HDT1023}$, $AgNb_{CAL823}$ and $AgNb_{HDT1023}$.

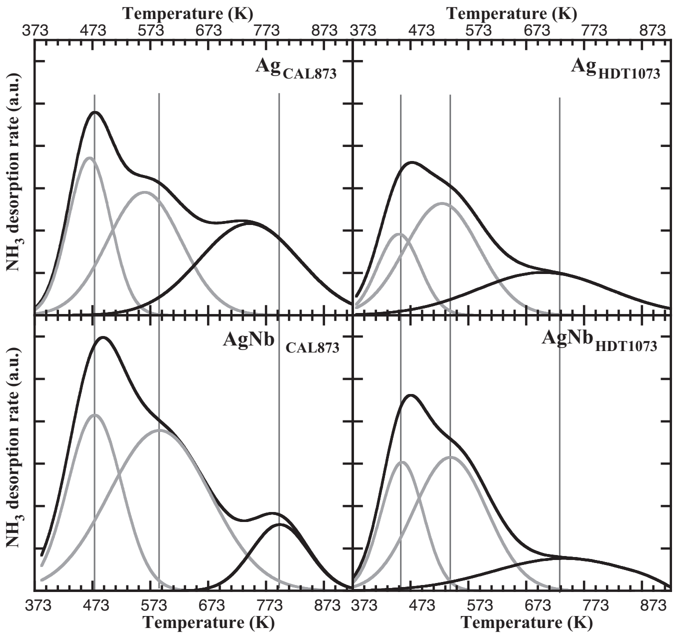

Fig. 8. NH3 TPD profiles of Ag_{CAL823}, $Ag_{HDT1023}$, $AgNb_{CAL823}$ and $AgNb_{HDT1023}$. Sample amount = 0.050 g, temperature ramp = 10 K/min from 373 to 903 K in He.

reduction of the total quantity of NH_3 was observed after HDT at 1023 K but the proportion of weak acid sites (NH_3 desorbing at low temperature) increased. By taking into account the loss of surface of these hydrotreated materials, the acid site density drastically increased and the highest value was obtained for $AgNb_{HDT1023}$ (Table 2).

4. Discussion and conclusions

Preparation of silver alumina based catalysts by non hydrolytic sol–gel method leads to mesoporous materials with high surface area. Despite these properties, the catalysts calcined at 823 K did not exhibit a high efficiency in the *n*-decane-SCR of NO. For having a high silver accessibility, obviously required for HC-SCR catalysis application, a treatment of the catalyst at high temperature is absolutely crucial for facilitating the silver migration and spreading, at maximum onto surface. The accessible silver particles are at maximum with a calcination temperature of at least 973–1023 K, thanks to silver high mobility. Migration of Ag to the surface was also reported occurring at low temperatures in solids with ion-implanted silver in lithia-alumina-silica glass [52]. XPS results of our samples show an increase of the Ag/Al ratio upon heating above 823 K. Moreover, the presence of a high concentration of water vapour during this thermal treatment has a positive effect on the SCR activity. We have recently shown that highly dispersed silver supported alumina catalysts can be prepared by heating, at a temperature between 903 and 948 K, a mixture of alumina and silver oxide in an oxidizing gas containing a water vapour concentration higher than 5.0 mol% [36]. The role of water is both to disperse and to anchor silver on the alumina surface. By considering this latter point and the sol–gel method used in this study, the effect of both temperature and water vapour presence in the calcination gas may be schematised according to Scheme 1.

As expected, a higher temperature of thermal treatment, for example 1023 K, induced a strong loss of surface area. Nevertheless, the resulting mesoporous materials have kept good structural properties. Despite this loss of surface area, hydrotreated materials exhibit a higher HC-SCR of NO activity at lower temperatures than the calcined catalysts. It should be underlined that this loss

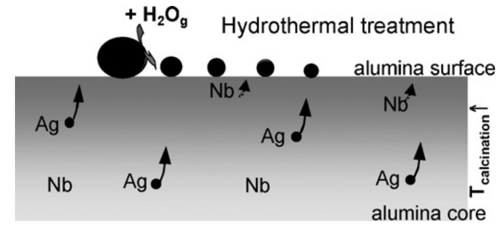

Scheme 1. Schematic migration of silver upon thermal and hydrothermal treatment.

of BET surface area is accompanied by a decrease of the quantity of acid sites as shown by measurements NH_3-TPD. But the density of acid sites increases. The better density is obtained for the catalyst containing niobium and hydrotreated at 1023 K. It is known that the acidic properties are one of the primordial factors for SCR activity improvement. According to Shimizu et al. [53], acidity of alumina support is one of the controlling factors for the SCR and these authors have reported a good correlation between SCR activity and the acid site density. They found the better activity for a modified Ag/alumina catalyst exhibiting the higher acid site density, i.e. 2.75 $\mu mol/m^2$. This value is very close to that observed for our best AgNb catalysts, i.e. 2.87 $\mu mol/m^2$.

Based on the UV–vis characterization, Sultana et al. [40] have correlated the activity of NO reduction to the presence of $Ag_n^{\delta+}$ clusters and acidity of Al_2O_3 support which was found to be one of the important parameter in promoting the formation and stabilization of $Ag_n^{\delta+}$ clusters. On the more active AgNb catalyst, where the starting silver content was fixed to 2 wt%, the average silver cluster size was, as determined by TEM, around 10 nm which is in agreement with previous studies [37,54–58] since smaller silver clusters are in stronger interaction with alumina support favouring thus the stabilization of oxidized (Ag^+) state.

Acknowledgements

This work was supported by the Fonds unique interministériel pôle AUTOMOBILE HAUT DE GAMME/AXELERA through the REDNOx project established and managed by PEUGEOT SA (G. Blanchard and S. Rousseau).

References

[1] R. Foo, N. Cortes Felix, Platinum Metals Review 53 (2009) 164.
[2] P. Granger, V.I. Parvulescu, Chemical Reviews 111 (2011) 3155.
[3] T. Miyadera, K. Yoshida, Applied Catalysis B 2 (1993) 199.
[4] T. Miyadera, K. Yoshida, Chem. Lett. 22 (1993) 1483.
[5] Y. Yoshida, G. Marumatsu, A. Abe, N. Irite, US Patent 5,589,432 (1996).
[6] J.P. Breen, R. Burch, C. Hardacre, C.J. Hill, B. Krutzsch, B. Bandl-Konrad, E. Jobson, L. Cider, P.G. Blakeman, L.J. Peace, M.V. Twigg, M. Preis, M. Gottschling, Applied Catalysis B: Environmental 70 (2007) 36.
[7] S.T. Korhonen, A.M. Beale, M.A. Newton, B.M. Weckhuysen, Journal of Physical Chemistry C 115 (2011) 885.
[8] K.-I. Shimizu, A. Satsuma, T. Hattori, Applied Catalysis B: Environmental 25 (2000) 239.
[9] L.-E. Lindfors, K. Eränen, F. Klingstedt, D.Yu. Murzin, Topics in Catalysis 28 (2004) 185.
[10] V. Houel, P. Millington, R. Rajaram, A. Tsolakis, Applied Catalysis B: Environmental 73 (2007) 203.
[11] K.A. Bethke, H.H. Kung, Journal of Catalysis 172 (1997) 93.
[12] A. Abe, N. Aoyama, S. Sumiya, N. Kakuta, K. Yoshida, Catalysis Letters 51 (1998) 5.
[13] S. Sumiya, M. Saito, H. He, Q.C. Feng, N. Takezawa, K. Yoshida, Catalysis Letters 50 (1998) 87.
[14] H. He, R.D. Zhang, Y.B. Yu, J.F. Liu, Chinese Journal of Catalysis 24 (2003) 788.
[15] E.F. Iliopoulou, A.P. Evdou, A.A. Lemonidou, I.A. Vasalos, Applied Catalysis A 274 (2004) 179.
[16] H. He, Y.B. Yu, Catalysis Today 100 (2005) 37.
[17] T.E. Hoost, R.J. Kudla, K.M. Collins, M.S. Chattha, Applied Catalysis B: Environmental 13 (1997) 59.
[18] F.C. Meunier, J.P. Breen, V. Zuzaniuk, M. Olsson, J.R.H. Ross, Journal of Catalysis 187 (1999) 493.

[19] K. Shimizu, J. Shibata, H. Yoshida, A. Satsuma, T. Hattori, Applied Catalysis B: Environmental 30 (2001) 151.
[20] L.E. Lindfors, K. Eranen, F. Klingstedt, D.Y. Murzin, Topics in Catalysis 28 (2004) 185.
[21] H. Kannisto, H. Härelind Ingelsten, M. Skoglundh, Journal of Molecular Catalysis A: Chemical 302 (2009) 86.
[22] N. Bogdanchikova, F.C. Meunier, M. Avalos-Borja, J.P. Breen, A. Prstryakov, Applied Catalysis B 36 (2002) 287.
[23] E. Seker, J. Cavataio, E. Gulari, P. Lorpongpaiboon, S. Osuwan, Applied Catalysis A: General 183 (1999) 121.
[24] T. Sato, S. Goto, Q. Tang, S. Yin, Journal of Materials Science 43 (2008) 2247.
[25] V.I. Pârvulescu, B. Cojocaru, V. Pârvulescu, R. Richards, Zhi Li, C. Cadigan, P. Granger, P. Miquel, C. Hardacre, Journal of Catalysis 272 (2010) 92.
[26] T. Nakatsuji, R. Yasukawa, K. Tabata, K. Ueda, M. Niwa, Applied Catalysis B 17 (1998) 333.
[27] Z. Li, M. Flytzani-Stephanopoulos, Journal of Catalysis 182 (1999) 313.
[28] R. Burch, J.P. Breen, F.C. Meunier, Applied Catalysis B 39 (2002) 283.
[29] M. Richter, M. Langpape, S. Kolf, G. Grubert, R. Eckelt, J. Radnik, M. Schneider, M.M. Pohl, R. Fricke, Applied Catalysis B 36 (2002) 261.
[30] N. Bogdanchikova, F.C. Meunier, M. Avalos-Borja, J.P. Breen, A. Pestryakov, Applied Catalysis B 36 (2002) 287.
[31] M. Yamaguchi, I. Goto, Z.M. Wang, M. Kumagai, Studies in Surface Science and Catalysis 121 (1999) 371.
[32] H.-W. Jen, Catalysis Today 42 (1998) 37.
[33] T. Furusawa, K. Seshan, J.A. Lercher, L. Lefferts, K. Aika, Applied Catalysis B 37 (2002) 205.
[34] A. Keshavaraja, X. She, M. Flytzani-Stephanopoulos, Applied Catalysis B 27 (2000) L1.
[35] A. Martínez-Arias, M. Fernández-García, A. Iglesias-Juez, J.A. Anderson, J.C. Conesa, J. Soria, Applied Catalysis B 28 (2000) 29.
[36] C. Petitto, G. Delahay, Catalysis Letters 142 (2012) 433.
[37] K.-I. Shimizu, A. Satsuma, Physical Chemistry Chemical Physics 8 (2006) 2677.
[38] K. Sato, T. Yoshinari, Y. Kintaichi, M. Haneda, H. Hamada, Catalysis Communications 4 (2003) 315.
[39] K. Shimizu, M. Hashimoto, J. Shibata, T. Hattori, A. Satsuma, Catalysis Today 126 (2007) 266.
[40] A. Sultana, M. Haneda, T. Fujitani, H. Hamada, Catalysis Letters 114 (2007) 96.
[41] S.A. Solov'ev, Ya P. Kurilets, S.N. Orlik, Theoretical and Experimental Chemistry 39 (2003) 58.
[42] J. Datka, A.M. Turek, J.M. Jehng, I.E. Wachs, Journal of Catalysis 135 (1992) 186.
[43] C. Petitto, P.H. Mutin, G. Delahay, Topics in Catalysis (2013).
[44] P.H. Mutin, A. Vioux, Chemistry of Materials 21 (2009) 582.
[45] V. Lafond, P.H. Mutin, A. Vioux, Chemistry of Materials 16 (2004) 5380.
[46] D.P. Debecker, K. Bouchmella, C. Poleunis, P. Eloy, P. Bertrand, E.M. Gaigneaux, P.H. Mutin, Chemistry of Materials 21 (2009) 2817.
[47] S. Acosta, R. Corriu, D. Leclercq, P.H. Mutin, A. Vioux, Journal of Sol–Gel Science and Technology 2 (1994) 25.
[48] C. Petitto, H.P. Mutin, G. Delahay, Chemical Communications 47 (2011) 10728.
[49] J.A. Moulijn, A.E. van Diepen, F. Kapteijn, Applied Catalysis A: General 212 (2001) 3.
[50] T. Nakatsuji, R. Yasukawa, K. Tabata, K. Ueda, M. Niwa, Applied Catalysis B: Environmental 17 (1998) 333.
[51] K.S.W. Sing, D.H. Everett, R.A.W. Haul, L. Moscou, R.A. Pierotti, J. Rouquerol, T. Siemieniewska, Pure and Applied Chemistry 57 (1985) 603.
[52] G.W. Arnold, J.A. Borders, Journal of Applied Physics 48 (1977) 1488.
[53] K. Shimizu, M. Hashimoto, J. Shibata, T. Hattori, A. Satsuma, Catalysis Today 126 (2007) 266.
[54] T. Furusawa, K. Seshan, J.A. Lercher, L. Lefferts, K. Aika, Applied Catalysis B 37 (2002) 205.
[55] M. Richter, U. Bentrup, E. Eckelt, M. Schneider, M.-M. Pohl, R. Fricke, Applied Catalysis B 51 (2004) 261.
[56] P. Zasama, L. Capek, H. Drobná, Z. Sobalik, J. Dedecek, K. Arve, B. Wichterlová, Journal of Catalysis 232 (2005) 302.
[57] B. Wichterlová, P. Zasama, J.P. Breen, R. Burch, C.J. Hill, L. Capek, Z. Sobalik, Journal of Catalysis 235 (2005) 195.
[58] J.P. Breen, R. Burch, C. Hardcare, C.J. Hill, Journal of Physical Chemistry B: Letters 109 (2005) 4805.